

CHAPTER 13

# Temporal dynamics of cortical sources underlying spontaneous and peripherally evoked slow waves

Brady A. Riedner<sup>†,‡,§,\*</sup>, Bradley K. Hulse<sup>†</sup>, Michael J. Murphy<sup>†,‡</sup>, Fabio Ferrarelli<sup>†</sup> and Giulio Tononi<sup>†</sup>

<sup>†</sup> Department of Psychiatry, University of Wisconsin-Madison, Madison, WI, USA

<sup>‡</sup> Neuroscience Training Program, University of Wisconsin-Madison, Madison, WI, USA

<sup>§</sup> Clinical Neuroengineering Training Program, University of Wisconsin-Madison, Madison, WI, USA

**Abstract:** Slow waves are the most prominent electroencephalographic feature of non-rapid eye movement (NREM) sleep. During NREM sleep, cortical neurons oscillate approximately once every second between a depolarized upstate, when cortical neurons are actively firing, and a hyperpolarized downstate, when cortical neurons are virtually silent (Destexhe et al., 1999; Steriade et al., 1993a, 2001). Intracellular recordings indicate that the origins of the slow oscillation are cortical and that corticocortical connections are necessary for their synchronization (Amzica and Steriade, 1995; Steriade et al., 1993b; Timofeev and Steriade, 1996; Timofeev et al., 2000). The currents produced by the near-synchronous slow oscillation of large populations of neurons appear on the scalp as electroencephalogram (EEG) slow waves (Amzica and Steriade, 1997).

Despite this cellular understanding, questions remain about the role of specific cortical structures in individual slow waves. Early EEG studies of slow waves in humans were limited by the small number of derivations employed and by the difficulty of relating scalp potentials to underlying brain activity (Brazier, 1949; Roth et al., 1956). Functional neuroimaging methods offer exceptional spatial resolution, but lack the temporal resolution to track individual slow waves (Dang-Vu et al., 2008; Maquet, 2000). Intracranial recordings in patient populations are limited by the availability of medically necessary electrode placements and can be confounded by pathology and medications (Cash et al., 2009; Nir et al., 2011; Wenneberg 2010).

Source modeling of high-density EEG recordings offers a unique opportunity for neuroimaging sleep slow waves. So far, the results have challenged several of the influential topographic observations about slow waves that had persisted since the original EEG recordings of sleep. These recent analyses revealed that individual slow waves are idiosyncratic cortical events and that the negative peak of the EEG slow

---

\*Corresponding author.

Tel.: +1-608-262-7128; Fax: +1-608-231-9011

E-mail: riedner@wisc.edu

wave often involves cortical structures not necessarily apparent from the scalp, like the inferior frontal gyrus, anterior cingulate, posterior cingulate, and precuneus (Murphy et al., 2009). In addition, not only do slow waves travel (Massimini et al., 2004), but they often do so preferentially through the areas comprising the major connectional backbone of the human cortex (Hagmann et al., 2008). In this chapter, we will review the cellular, intracranial recording, and neuroimaging results concerning EEG slow waves. We will also confront a long held belief about peripherally evoked slow waves, also known as K-complexes, namely that they are modality independent and do not involve cortical sensory pathways. The analysis included here is the first to directly compare K-complexes evoked with three different stimulation modalities within the same subject on the same night using high-density EEG.

**Keywords:** slow oscillation; source modeling; K-complex; neuroimaging; electroencephalography.

## Introduction

In 1924, Hans Berger produced the first recordings of brain activity from the human scalp (Millett, 2001). He called the recordings “Elektrenkephalogram” which literally means a “writing” of the electrical activity of the brain. Berger demonstrated that these “writings” contained waveforms that changed in response to a change in human brain state (Berger, 1929). The electroencephalogram (EEG) was soon being applied to the most profound, regularly occurring alteration in the state of the human brain—*sleep*.

Researchers examining sleep during the early days of EEG were primarily concerned with the codification of behavioral states. These early studies revealed that during the deepest stage of sleep, when subjects were least arousable, scalp EEG recordings were dominated by high-amplitude slow waves. In this sense, large amplitude slow or “delta” waves were exemplary in discriminating the transition from waking to light and then deeper stages of sleep (Blake and Gerard, 1937; Davis et al., 1938). Intriguingly, these researchers’ attempts to measure arousability also led to another discovery. External stimuli delivered during sleep can often induce waves in the human brain that closely resemble spontaneously generated slow waves, particularly those isolated versions present during lighter sleep (Blake and

Gerard, 1937; Davis et al., 1939; Loomis et al., 1938). Occurring approximately once every second with amplitudes of up to several hundred microvolts, sleep slow waves, whether spontaneous or evoked, are the largest EEG graphoelements generated by the normally functioning human brain.

Undoubtedly though, EEG pioneers were curious about more than just the behavioral state implications of the massive slow wave potentials repeatedly appearing during sleep. However, what additional information could EEG offer, in addition to the fine temporal precision that makes it useful to characterize the various oscillatory activities endogenously produced by the brain? Several influential and enduring observations about where and how slow waves were produced came from these seminal EEG studies, despite their limited spatial coverage. Today the landscape of human brain study is much different. Computerized axial tomography, positron emission tomography (PET), magnetic resonance imaging (MRI), and other technologies offer a noninvasive view into both structural and functional human brain anatomy with unparalleled spatial resolution. These technologies have ushered in the era of neuroimaging and have afforded tremendous advantages to expand our knowledge of brain activity during sleep. In this chapter, we will review three cardinal observations regarding EEG sleep slow waves

and see how technological advances have influenced and enriched our understanding of them. In particular, we will highlight recordings with high-density electroencephalogram (hd-EEG), which uniquely combines the requisite temporal precision to examine sleep slow waves with the opportunity to image the entire cortex. Additionally, we have included some new hd-EEG data which challenges the notion that evoked K-complexes are “nonspecific” responses of the sleeping brain to peripheral stimulation, as is generally assumed.

## Where are slow waves?

### *Traditional EEG studies*

Initial EEG recordings were done with just a few electrodes placed along the midline or on either side of the vertex, as is the case even today for routine clinical polysomnographies. Such limited electrode placements allowed researchers to distinguish the frequency shifts that characterize sleep stages, but seemingly offered little hope in terms of localization of brain sources. Despite these technological limitations, there were several researchers who conducted careful examinations into the “topography” of sleep slow waves. The two most thorough of these studies were done by [Brazier \(1949\)](#) on spontaneous waves and by [Roth et al. \(1956\)](#) on evoked K-complex slow waves.

When EEG sleep slow waves were first reported, the most common observation was that they were large, frontocentral waves, in contrast to the much smaller and occipital alpha waves found during waking ([Loomis et al., 1938](#)). By changing the configuration of up to eight electrodes at any given time, Brazier was able to hypothesize about the electrical fields which could be responsible for slow waves ([Brazier, 1949](#)). She reasoned that the electrical fields producing slow waves were likely to result from dipoles orientated perpendicular to the scalp, in line with the current understanding of the cortical

generation of EEG from pyramidal neural sheets capable of producing macroscopic electrical fields ([Lopes da Silva, 2004](#); [Nunez and Srinivasan, 2005](#)). She also concluded that slow waves had two prominent foci: a precentral focus corresponding approximately with Brodmann Area 6 and a far frontal focus thought to include Brodmann Area 9. By tightly spacing electrodes across and perpendicular to the midline of the presumed precentral focus, foreshadowing the dense array EEG recordings of the future, she observed phase reversals which she attributed to the simultaneous discharge of homologous bilateral precentral regions. While providing evidence that individual slow waves are not completely uniform and can occur in different places, her conclusions points to one of the obvious limitations of scalp-recorded EEG. Although it is often reasonable to assume that EEG waveforms reflect the currents in the directly underlying cortex, this assumption is not supported mathematically ([Gotman, 2003](#); [Nunez and Srinivasan, 2005](#)). The currents that give rise to EEG scalp potentials are only relayed to the surface through volume conduction. Thus local potentials can be generated by sources that are distant to the recording electrodes ([Michel et al., 2004](#); [Nunez and Srinivasan, 2005](#)). This is not to say that Brazier did not understand the physics inherent to the problem of scalp EEG. Recording from a specially designed nasopharyngeal electrode, Brazier ruled out that the far frontal slow wave potentials were actually the result of activity from the base of the brain, distant from her original recording electrodes. Still, in the human brain there are other deep cortical areas which are far away from the scalp (like the cingulate gyrus) but are still capable of producing large macroscopic field potentials at the surface.

The possibility of a deep current source was considered by [Roth et al. \(1956\)](#). After describing the similar topography between auditory, visual, or tactile evoked K-complexes and spontaneously generated sleep slow waves, the authors examined individual components of the evoked

K-complex. As expected, the authors concluded that neither the initial positive vertex component nor the later negative, anterior component were consistent with involvement of the primary sensory pathways, as suggested by [Brazier \(1949\)](#) and others. Yet in contrast to Brazier, the authors pointed out that the topography of the K-complex (presumably either component) could be the result of a deep electrical source in the cingulate gyrus, consistent with an earlier suggestion which the authors attribute to [Gastaut \(Gastaut et al., 1953; Roth et al., 1956\)](#), although [Roth et al. \(1956\)](#) favored the involvement of a diffuse projection system from an unknown subcortical center, a point which will be discussed later in this chapter. This consideration acknowledges another important fact about scalp-recorded EEG. Namely that while different scalp voltage topographies must necessarily be produced by a different pattern of underlying currents, potential measurements taken on the surface of a conductor can never uniquely specify the configuration of current inside the conductive volume ([Hamalainen et al., 1993; von Helmholtz, 2004](#)). Therefore, both [Brazier \(1949\)](#) and [Roth et al. \(1956\)](#) concluded that animal models would be necessary to resolve the ambiguity in terms of sources of activity.

### ***The slow oscillation***

Indeed, probably the most significant advance in understanding slow waves did come from animal research when in the early 1990s the Steriade laboratory identified the slow oscillation in the membrane potential of ketamine/xylazine anesthetized cats ([Steriade et al., 1993a](#)). This cellular phenomenon consists of a depolarized upstate characterized by irregular neuronal firing with rates that can be as high as during wakefulness, and a hyperpolarized downstate when neuronal silence predominates ([Destexhe et al., 1999; Steriade et al., 1993a, 2001](#)). Subsequent research has provided a wealth of information about the

cellular mechanisms underlying the slow oscillation. While this is not the proper place for an exhaustive review of this literature, as several of the chapters in this volume cover the most recent understanding of these mechanisms, several key results should be highlighted.

First and foremost, the slow oscillation is a cortical phenomenon. Although the thalamus may contribute to shaping the rhythm, isolated slabs of cortex are capable of generating the slow oscillation ([Crunelli and Hughes, 2010; Timofeev et al., 2000](#)). The slow oscillation does not, instead, occur in the decorticated thalamus ([Timofeev and Steriade, 1996](#)). Further, disruption of corticocortical connections prevents the synchronization of these oscillations ([Amzica and Steriade, 1995](#)). A second point is that these near-synchronous oscillations of large populations of cortical neurons between depolarized and hyperpolarized states during sleep are the underlying cellular correlate of scalp-recorded large EEG slow waves and K-complexes ([Amzica and Steriade, 1997, 1998b; Destexhe et al., 1999](#)). If cortical neurons are then responsible for generating and maintaining the slow oscillation which produce scalp-level EEG slow waves, the question then becomes which cortical neurons? Originally it was proposed by Steriade and others that all cortical neurons participate in the slow oscillation, but this suggestion was based on limited intracellular electrode placements ([Amzica and Steriade, 1998a; Steriade et al., 1993a](#)). However, this notion has recently received significant confirmation with the advent of simultaneous multisite intracellular recordings ([Volgushev et al., 2006](#)) which have shown that during the conditions of sleep-like anesthesia, all types of cortical cells recorded and all locations participate in the slow oscillation, with only the occasional cortical neuron skipping a cycle of the oscillation.

Still, what can be made of the fact that EEG recordings of slow waves in humans during natural sleep do not show a uniform distribution on the scalp even with limited channel recordings? Some

answers can come from unique datasets consisting of sleep recordings from multiregion simultaneous scalp and intracerebral depth EEG electrodes implanted in neurosurgical patients (Nir et al., 2011). These data, including single-unit recordings from extracellular microwires, reveal that although some individual slow waves involve a number of separate brain regions concurrently, many slow waves are confined to local brain regions, unlike those recorded in animals during ketamine–xylazine induced anesthesia. Researchers have also turned to several of the currently available noninvasive methods for imaging the human brain that are not limited by available patients and surgically necessary electrode placements and allow the entire brain (or cortex) to be imaged simultaneously.

### ***Positron emission tomography***

The majority of studies using imaging techniques to examine slow waves in humans have used PET combined with EEG to show how regional cerebral blood flow or metabolism changes as a function of slow wave sleep. These studies typically compare non-rapid eye movement (NREM) sleep scans versus waking scans after accounting for the global activity decreases accompanying sleep to show regionally specific areas. As in the topography of EEG sleep slow waves, the pattern of deactivations suggest that the cortex does not behave homogeneously during NREM sleep. Generally, frontal cortical areas like the orbital and anterior cingulate cortex, as well as areas in the parietal cortices, the posterior cingulate, precuneus, and occasionally insular cortex have shown consistent decreases in blood flow during NREM sleep (see Maquet, 2000 for a review). The general interpretation from these studies is that decreases of blood flow during NREM likely means that these areas have the highest proportion of cortical neurons participating in EEG slow waves (Maquet, 2000). Metabolism scans using [ $^{18}\text{F}$ ]fluoro-2-deoxy-D-glucose ([ $^{18}\text{F}$ ]FDG) during

NREM sleep have revealed slightly different results in that no decreases in metabolism were found in the orbitofrontal, cingulate, or insular cortices, and some relative increases in metabolism were observed in the anterior cingulate (Nofzinger et al., 2002). The reason for these discrepancies is unknown but they may result from methodological differences between these types of studies. For example, the [ $^{18}\text{F}$ ]FDG scans involve imaging the result of a 20-min uptake period at the beginning of the night during which the subject spent the majority of time in stage 2 NREM sleep as indicated by EEG, but which also necessarily included any time spent awake or in lighter stages of sleep (Nofzinger, 2005; Nofzinger et al., 2002). Unfortunately, these authors did not attempt to correlate the number of slow waves observed during the uptake time with metabolism. PET blood flow studies, instead, have better temporal resolution and allow verification of the EEG stage at the time of the scan. Thus, two more recent studies using PET blood flow scans have shown that the medial frontal, anterior cingulate, orbitofrontal areas are most negatively correlated with EEG delta (1.5–4.0 Hz) power (Dang-vu et al., 2005; Hofle et al., 1997). The insula and precuneus also showed a negative correlation with delta EEG power. As slow waves are the main contributors to delta EEG, these results suggest that the deactivation in these areas is likely related to these areas participation in the slow neuronal oscillation. Similar results were also obtained using EEG combined with functional magnetic resonance imaging (fMRI) (Kaufmann et al., 2006).

### ***Event-triggered fMRI***

An important contribution to the neuroimaging of human slow waves has come from event-related EEG-fMRI designs. By triggering the scans on the appearance of slow waves, in this case the peak of the EEG negativity, researchers were able to

more directly examine the brain areas involved in sleep slow waves (Dang-vu et al., 2008). As opposed to simply correlating the scans with delta activity, the researchers compared the resulting high spatial resolution images of individual slow waves with a baseline of NREM sleep when there are no slow waves. The authors instead found relative differences in the inferior and middle frontal gyri, as well as the precuneus and posterior cingulate cortex related to the presence of slow waves, suggesting that these areas are the most involved in slow waves. The results emphasize that individual slow waves do not uniformly involve the entire cortex. The cortical areas most involved in slow waves also show a substantial overlap with the default mode network, a set of brain areas that deactivate when subjects perform tasks (Raichle and Snyder, 2007; Raichle et al., 2001). However, the differences these authors found in these areas were all increases relative to baseline and did not depend on the particular phase of the slow wave. This fact points out one of the limiting factors of fMRI which is that the temporal resolution is on the order of seconds. Whether the authors triggered on the EEG negative peak, presumably integrating over the subsequent upstate, or triggered on the positive peak of the EEG slow wave, the results were the same. This result may be due to the fact that the temporal resolution of fMRI is on the order of seconds. Unquestionably though, the results highlight the fact that slow waves do not homogeneously affect the cortex and particularly involve cortical areas that are consistent with default mode structures.

### ***High-density EEG***

As mentioned earlier, scalp-level EEG explorations into slow waves have been hampered by two critical limitations: (1) the lack of spatial resolution offered by limited channel recordings and (2) the indeterminate nature of source localization from scalp voltage potentials. However, these restrictions have lessened in the

past decade due to the rapid improvement of computer processing speed and the decreased costs associated with high volume data collection and storage. Thus, in recent years, hd-EEG recordings, which can incorporate hundreds of electrodes, have become increasingly common. In parallel, source modeling analysis techniques have become substantially more sophisticated, moving beyond the dipolar models that assume a small number of active sources, to distributed source models that make no assumptions about how many areas of the brain can be simultaneously responsible for given scalp potentials (Michel et al., 2004). In addition, hd-EEG is relatively inexpensive, is portable, and allows subjects to sleep in a natural environment without being sleep deprived, a common practice for other imaging experiments where scan time is expensive and subjects must be able to fall asleep motionless inside of a scanner (Nofzinger, 2005).

Admittedly, source modeling of EEG must still be predicated on certain assumptions. However, in regard to slow waves, the wealth of animal research and investigations with other imaging techniques bolster the ability to make reasonable choices and lend credence to the results obtained. For instance, distributed source models typically divide the brain into a number of cortical voxels based on the knowledge that only the synchronous activity of large numbers of cortical pyramidal neurons, arranged in parallel, are sufficient to produce scalp potentials capable of being recorded from the scalp (Lopes da Silva, 2004; Nunez and Srinivasan, 2005). As compared to Roth et al. (1956) who proposed a subcortical source for EEG slow waves based on the observation of a widespread electrical field, we now know, particularly from the animal literature, that the underlying feature of EEG slow waves is the near-synchronous slow oscillation of large populations of cortical neurons between depolarized and hyperpolarized states. We also know that the cortex is sufficient to initiate and maintain these oscillations (Amzica and



Steriade, 1995; Steriade et al., 1993b; Timofeev and Steriade, 1996; Timofeev et al., 2000). Therefore, the voxelation of the cortical gray matter as potential sources, typical in EEG source modeling, is a valid and reasonable assumption when applied to slow waves.

The results obtained by source modeling EEG slow waves are consistent with the available neuroimaging literature. In the most direct comparison to the recent EEG-fMRI results, we detected individual spontaneous slow waves during slow wave sleep and examined the average current associated with negative peak of the slow waves—a measure of the degree to which a certain area (source voxel) is involved in each slow wave (Murphy et al., 2009). The negative peak of the scalp-recorded EEG slow wave likely reflects the beginning of the transition from downstate to upstate and the resumption of neural firing (Contreras and Steriade, 1995; Destexhe et al., 1999; Volgushev et al., 2006; Vyazovskiy et al., 2009). As expected, the involvement of slow waves was not uniformly distributed in the cortex. On average, the cortical areas that were most involved in slow waves shared a marked overlap with the BOLD-fMRI results and included the left inferior frontal gyrus, the entire extent of the cingulate gyrus (from anterior to posterior), the precuneus and the insula. Based on the millisecond temporal resolution of EEG, the relative involvement of specific cortical areas around this time point indicates that they are not just associated with slow waves in general, as can be derived from the EEG-fMRI results, but that they are specifically involved during the down to up state transition.

### Are slow waves synchronous?

In addition to noting their apparent frontal location, pioneering EEG sleep researchers identified slow waves as synchronous at remote brain regions (Blake et al., 1939; Davis et al., 1938). This observation led them to suggest that

sleep slow waves were a global cortical event. More recent research, exploiting the advanced techniques described above (Dang-Vu et al., 2008; Maquet, 2000; Murphy et al., 2009; Nir et al., 2011) has consistently indicated that EEG slow waves are not always global in the sense that specific brain regions are not involved or do not participate equally in every slow wave. Still, despite the regional specificity of EEG slow waves, whenever and wherever they occur, do they occur synchronously?

In 2004, Massimini et al. dispelled the notion of EEG sleep slow waves as globally synchronous (Massimini et al., 2004). Taking advantage of the temporal resolution of EEG and the dense channel array to track the negative peak of individual slow waves, this scalp-level analysis demonstrated for the first time that individual sleep slow waves propagate uniquely across the cortex from distinct origins (Massimini et al., 2004). Importantly, the pattern of propagation was shown to have a preferred anterior–posterior direction, and to be consistent across nights in the same subject.

Capitalizing on this work, we used source modeling of EEG slow waves to determine the cortical correlates of traveling waves (Murphy et al., 2009). We revealed that the two origin hotspots apparent in the scalp data reflected cortical origin hotspots in the left insula and the cingulate gyrus. As was the case for cortical involvement, these areas were not easily predictable from the scalp data alone. We also found that although each wave was an idiosyncratic event differentially impacting a distinct subset of cortical areas, there was a preferential pattern of traveling. Analysis of the streamline pathways, a measure of the likely propagation path of individual slow waves, demonstrated that slow waves traveling in the anterior–posterior direction typically do so along a mesial slow wave highway that bears a remarkable resemblance to the anatomical connectivity backbone revealed by diffusion spectrum imaging (Hagmann et al., 2008). Significant evidence exists that information from the periphery reaches the cortex even during NREM

sleep (Hennevin et al., 2007; Issa and Wang, 2008; Massimini et al., 2003; Portas et al., 2000; Rosanova and Timofeev, 2005). Whether downstates propagating along this highway are a contributing factor in the curtailing of information transmission during sleep is unknown but is an intriguing possibility. Further, the degree to which mapping sleep slow waves may offer an inexpensive and easily accessible adjunct to the sophisticated fiber tracking methods available with MRI remains to be seen.

Unfortunately, the temporal resolution of other noninvasive neuroimaging techniques in humans does not allow for direct comparisons with this work. However, multisite intracellular recordings in ketamine/xlyazine anesthetized cats provided additional evidence for the notion that slow oscillations propagate from distinct origin sites and have a preferred anteroposterior direction of travel (Chauvette et al., 2010; Volgushev et al., 2006). Simultaneous recordings from 8 to 12 distant brain structures from depth electrodes in neurosurgical patients, confirmed the prominent anterior–posterior direction of slow wave propagation (Nir et al., 2011). Although obviously limited in availability, these datasets (see also Cash et al., 2009) provide another invaluable contribution to the understanding of slow waves. It should also be noted that the areas most often involved in the intracranially recorded slow waves included medial prefrontal areas like the anterior cingulate, consistent with source modeled hd-EEG slow waves (Murphy et al., 2009). As a caveat, although the majority of evidence from several different techniques support the involvement of deep midline structures like the cingulate in sleep slow waves, a different study using primarily subdural strip electrodes in epileptic patients arrived at different conclusions, failing to find evidence for deep midline involvement in slow waves or evidence for traveling waves (Wennberg, 2010). Discrepancies could be the result of the type of recording (field potential recordings from strip electrodes placed on the cortical surface versus

depth electrode and microwire recordings), the type of slow waves being examined (stage 2 spontaneous K-complex waves versus slow waves throughout NREM sleep), or differences in the patient populations, as well as other methodological differences. In addition to a preferred anterior–posterior direction of travel, a recent study using voltage sensitive dyes suggests that interhemispheric connections between homologous regions of the cortex may be implicated in the propagation of the slow oscillation (Mohajerani et al., 2010).

### **Are K-complexes nonspecific responses to peripheral stimulation?**

The term K-complex was originally used to describe the characteristic large potential waves following tone stimulation during sleep. These EEG waves lasted about a second and consisted of a “swing down” negativity of several hundred microvolts followed by a “swing up” positivity (Loomis et al., 1938). Isolated versions of these waves were also observed during lighter stages of sleep which did not appear to be elicited by any source outside the brain. These characteristic waves, both spontaneous and induced, were deemed “K-complexes” (Loomis et al., 1938). Although auditory stimulation was most effective in producing them, K-complexes were noted in response to a variety of different stimuli, all of which produced the same “diffuse, nonspecific, delayed electrical response” in the human brain (Davis et al., 1939). Later works, like the Roth paper, used several different types of stimuli but did not show direct comparisons, and with limited channel montages it is unlikely that any differences would have been easily observed. Colrain et al. (1999) and others gave the idea that K-complexes were the same, regardless of stimulation type more definitive support by examining the scalp topography of both auditory evoked and respiratory occlusion evoked K-complexes. In this study, the authors evoked K-complexes



either by means of auditory stimulation or through respiratory occlusion and recorded the responses with an extended EEG montage (29 channels). Respiratory occlusion, it should be noted, is a form of somatosensory stimulation. They then compared the average evoked response topography at each electrode between the two conditions and found no differences. The results of this study confirmed the similarity of the scalp topographies at the negative peak of the K-complex. In an excellent and thorough review of the K-complex literature by Colrain several years later (Colrain, 2005), which summarizes several of the studies also discussed in this chapter, the author emphasizes the notion that the K-complex is a modality independent, sleep specific response to stimulation, noting that the evoked K-complex does not involve sensory-relay thalamocortical pathways.

The degree to which the cortex receives information about peripheral stimulation during sleep has long been controversial. Most studies in humans have relied on evoked potential studies. These studies have consistently suggested that while the early components, typically thought to reflect brainstem or nerve conduction are preserved during sleep, later components are usually disrupted (for a review, see Bastuji and Garcia-Larrea, 1999). The lack of brain responsiveness during sleep is usually attributed to a thalamic gating (Steriade et al., 1990). While there have been few stimulation studies in naturally sleeping animals (for reviews, see Hennevin et al., 2007; Velluti, 1997), one recent report suggests that in naturally sleeping monkeys there is preservation of responses from both primary and secondary auditory cortical area to acoustic stimulation (Issa and Wang, 2008). Other studies have shown that the phase of the cortical slow oscillation can be an important factor in determining the degree to which sensory information reaches the cortex (Massimini et al., 2003; Rosanova and Timofeev, 2005).

Neuroimaging techniques have also recently been used to address the issue of the degree of cortical response to sensory stimulation during sleep. A landmark study in this regard was published in *Neuron* by Portas et al. (2000). The auditory cortex activation observed during the presentation of the subject's name or a beep was remarkably conserved between waking and NREM sleep. In a study using fMRI and combined EEG-PET imaging, however, visual stimulation was shown to decrease activity in the occipital cortex and another study showed significant decreases in auditory cortex with tone stimulation using EEG-fMRI during NREM sleep compared to wakefulness (Born et al., 2002; Czisch et al., 2002). In contrast, an even more recent study by Czisch used EEG-fMRI and showed auditory cortical activation in response to tones, but only when the tones produced a K-complex (Czisch et al., 2009). Interestingly during the tone evoked K-complexes, activation was also found in middle frontal gyri and cingulate areas.

Given these recent results, we decided to revisit the notion that evoked K-complexes are entirely modality independent. Therefore, we source modeled hd-EEG recordings (256 channel HydroCel Geodesic Sensor Net, Electrical Geodesic Inc.) to directly compare the cortical sources of K-complexes evoked with three different kinds of stimulation: auditory (50 ms, 2000 Hz pure tones delivered through earphones or speakers); somatosensory (0.3 ms constant current squarewave pulses delivered to the median nerve of the dominant hand at intensities around motor but below pain threshold); and visual (stroboscopic flashes, 10  $\mu$ s duration, at or below the maximum flash intensity of 20 lumen-s/ft<sup>2</sup> placed approximately 3 ft away from the subject's face). In order to compare different modalities of K-complexes in the most direct manner possible, we employed a within subject, within night comparison of the responses. Two-minute blocks of the same stimulus modality were delivered with a 5 s within block interstimulus interval (ISI)

during sleep stages N2 and N3. In order to maximize the number of stimulation blocks within the night, we chose to use the minimum ISI which is still expected to be longer than the K-complex refractory period (Colrain, 2005). Stimulation blocks were separated by at least 1 min. The type of stimulation was pseudorandomly distributed throughout the night. Intensity of stimulation was manually modulated between blocks so as to maximize the chance to produce a K-complex without arousing the subject from sleep. Of the seven subjects (males age 22–36, two left-handed) who participated in the experiment, one subject was consistently aroused by the visual stimulation and another showed substantial high-amplitude, low-frequency artifact which precluded identification of K-complexes. Therefore, data from five subjects were included in the final analysis. Approximately 1000 total stimuli were delivered to each subject (mean = 1032, range 595–1379) and different modality stimulations were evenly distributed throughout the night. EEG was sampled at 1000 Hz, re-referenced to the average of the mastoids (originally referenced to the vertex) and band-passed filtered (0.1 Hz first order high pass, 0.5–40 Hz). Visually identified bad channels were replaced using spline interpolation. Responses were identified as K-complexes if there was a negative peak of at least 50  $\mu$ V in the butterfly plot of all 256 channels between 200 and 1100 ms after the stimulus and if the negative peak amplitude was larger than the activity in the 500 ms prior to the stimulation. Success for evoking K-complexes was similar to what has been previously reported (mean  $\pm$  range: auditory 32%  $\pm$  21–47%; somatosensory 17%  $\pm$  14–21%; visual 43%  $\pm$  33–55%). Surprisingly, visual stimulation was more successful than auditory or somatosensory stimulation in evoking K-complexes for four out of the five subjects.

Figure 1a–c shows EEG butterfly plot traces (all 256 channels overlaid) of the grand average across subjects for slow waves evoked by each stimulation modality. The largest component of

the average evoked response for the three different stimulations was a negative peak occurring between 400 and 700 ms. In the evoked potential literature, this peak is called the N550. Since the N550 peak is only evident in average responses during sleep that include K-complexes, it is commonly utilized as a means to investigate the characteristic differences between K-complexes across different stimulation conditions (Bastien et al., 2002). Our analyses initially focused on this peak, which is the EEG reflection of the cellular downstate evoked by stimulation. However, we also wanted to take advantage of the temporal resolution of EEG to further explore the time course of any topographical differences. Given the latency variability of the responses across conditions and subjects even after averaging, we segmented the evoked potential response for each subject and condition based on the evoked components observed during NREM sleep (Bastien et al., 2002). This segmentation applied to the grand averages is shown in Fig. 1a–c and included the P200 (0–300 ms auditory, 0–200 ms somatosensory, and 0–260 ms visual in the grand averages), the N350 (300–445 ms auditory, 200–315 ms somatosensory, 260–420 ms visual), N550 (445–775 ms auditory, 315–545 ms somatosensory, 420–650 ms visual), and the P900 components (900–1535 ms auditory, 1030–1560 ms somatosensory, 850–1580 ms visual).

In agreement with previous results, there was a clear similarity in the scalp topography of the N550 peak across stimulations (Fig. 1a'–c'). The relative scalp topography of the largest evoked negative peak for all three modalities had a hot spot of negativity centered near the approximate 10-10 location of AFz. However, the scalp topographies were not completely redundant, with the most obvious difference being that the negative peak hot spot extends to include Cz in the visual condition. To examine the cortical sources of the evoked K-complexes, we source modeled each time point of the average evoked response for each modality and each subject using

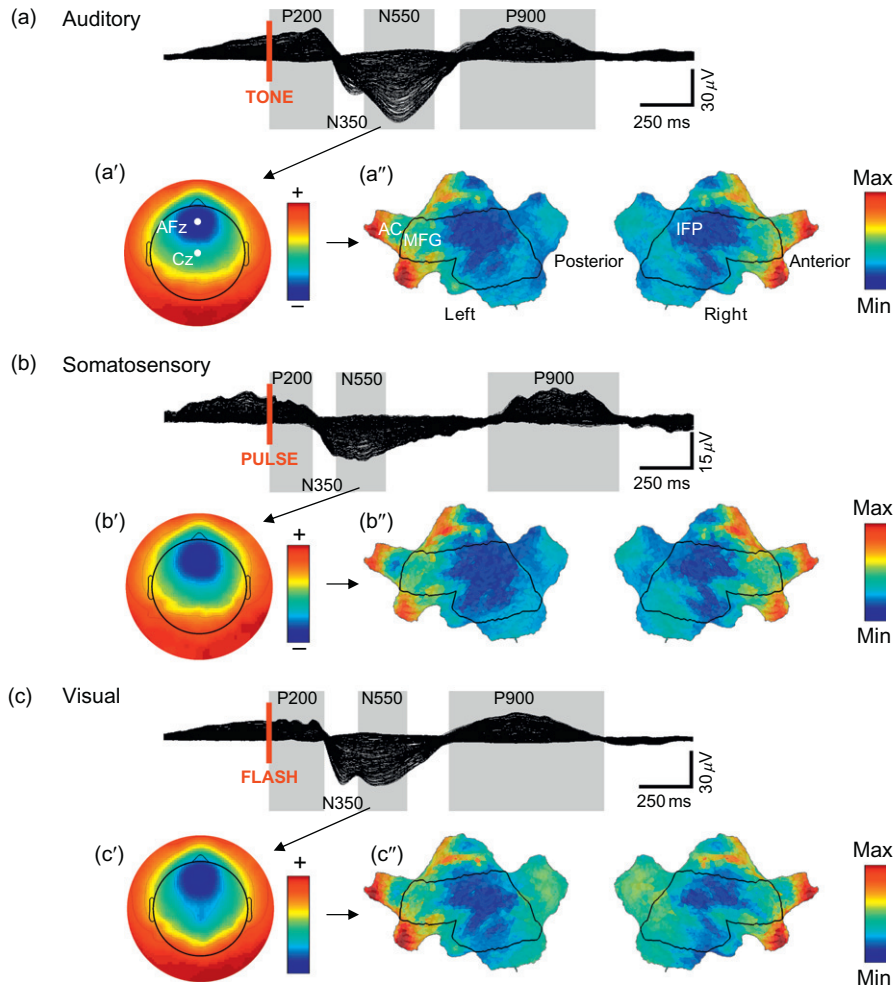


Fig. 1. Similarity of scalp and source topographies of K-complex responses. (a)–(c): Across subject grand average 256-channel EEG butterfly plot (overlaid traces) of the evoked response during sleep for each stimulation modality. Red line indicates the time of stimulation. Labeled boxes indicate time periods of evoked responses selected for comparison across modalities. (a')–(c'): Scalp topography for the N550 time periods. Each map is independently scaled in order to indicate relative topography. Red indicates positivity with respect to the average. Blue indicates negativity. 10–10 approximate locations of AFz and Cz are shown as white dots and are labeled accordingly. (a'')–(c''): Flat maps of the cortical sources for the N550 peak. Current sources were z-transformed for each time point before averaging across time. Median z-score current across subjects is displayed. Current hot spots (most current) indicated in red, cold spots in blue. AC, anterior cingulate; MFG, middle frontal gyrus; IPL, inferior parietal lobule.

a four-shell forward model consisting of 2447 cortical voxels and the standardized low resolution electromagnetic tomography inverse solution (sLORETA, Geosource 2.0) with Tikhonov

regularization ( $10^{-1}$ ). The source modeling technique used here was similar to what was previously utilized to examine spontaneous slow waves (Murphy et al., 2009) but removed the

necessity of using baseline data to normalize the results because the sLORETA constraint accounts for measurement and biological noise directly within the algorithm itself (Pascual-Marquis, 2002). To compare relative current source topographies across subjects, current sources for each time point were  $z$ -score transformed before averaging across time periods. Flat maps of the  $z$ -transformed cortical sources corresponding to the N550 peak time period are displayed in Fig. 1a''–c''. In terms of current source topography, the flat maps reveal that the current sources for the negative peak of the K-complex, like the scalp topographies, are relatively consistent across modalities, although a slight increase in current is present in occipital areas for K-complexes evoked by visual stimulation. Across stimulations, the cortical areas where the evoked K-complexes were most pronounced in terms of relative current across stimulation conditions were bilaterally in the anterior cingulate, middle frontal, inferior frontal, orbital, and rectal gyri. The largest current coldspot (minimal current) was the inferior parietal lobule. The topographic consistency of the N550 peak across stimulation modalities and the fact that primary sensory areas are not the areas with the largest amount of current generally confirms the notion that peripheral stimuli likely utilize a common mechanism for producing cortical slow waves that does not directly involve the primary sensory pathways (Bastien et al., 2002; Colrain, 2005; Roth et al., 1956).

Still, is there no role for the primary sensory pathways in peripherally evoked slow waves? In order to answer this question, we chose to directly compare the cortical sources with a more fine-grained analysis to explore whether the evoked K-complex slow wave responses were entirely sensory pathway independent. To do so, we used a nonparametric Quade test to compare cortical sources across stimulation conditions. The Quade test is an extension of the Wilcoxon signed ranks test for cases of multiple related conditions and is especially powerful when the

number of conditions is less than 5 (Conover, 1999). Each of the 2447 cortical source voxels for each subject was ranked according to the amount of relative ( $z$ -transformed) current for the three stimulation conditions. Essentially, the higher the current, the higher the rank. The Quade test establishes the statistical significance based on the consistency of these rankings across subjects. For statistically significant voxels, Quade rankings can be examined directly to determine the stimulation condition with the largest relative current compared to the other two (García et al., 2010). The rankings are also submitted to *post hoc* procedures to determine the significant differences for all possible comparisons.

The direct comparison of current sources at the negative peak of the evoked K-complex slow wave revealed that there are in fact cortical areas which show differences in relative current between stimulation conditions (Fig. 2b, c). Interestingly, not only are some cortical regions significantly different across the stimulation conditions, but the statistically different regions exhibit a pattern of relatively increased currents that suggests an obvious relationship with the type of stimulation. For instance, there is a left hemisphere area that includes Brodmann areas 17–19, comprising primary and secondary visual cortex, which is significantly different across stimulation modalities (Fig. 2b and c). Based on Quade rankings, the negative peak has the largest currents in this area when a K-complex is evoked by visual stimulation, compared to the other stimulations (Fig. 2b). *Post hoc* analysis of the Quade rankings confirms that visual stimulation in these areas is significantly larger than one or both of the other stimulation modalities (Fig. 2c). Other areas in the occipital gyrus were also different including portions of the posterior cingulate and precuneus and showed larger relative current peaks during the negative portion of the scalp EEG K-complex evoked by visual stimulation. Similarly, a large cortical area that included parts of the primary somatosensory and motor cortices and extended anteriorly to include the supplementary motor

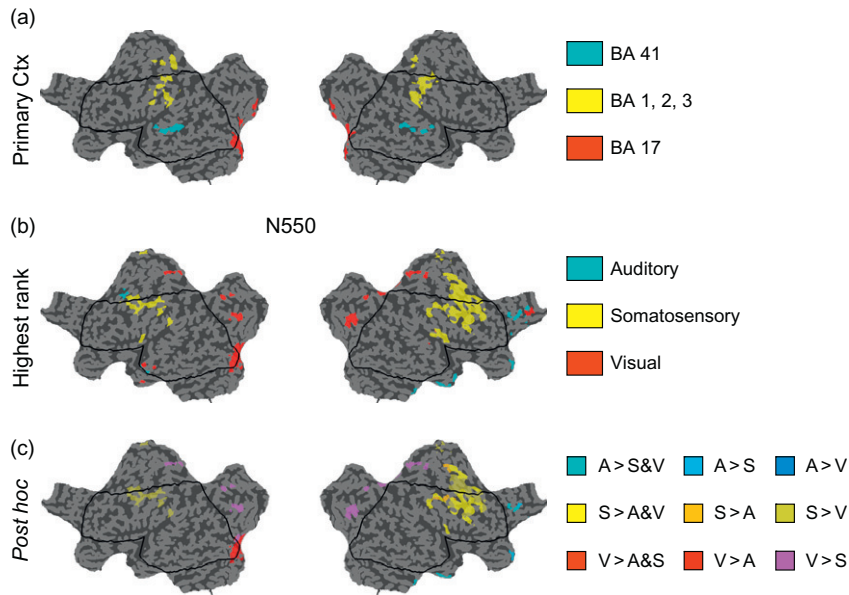


Fig. 2. N550 peak shows modality specific differences in cortical sources that include primary cortical areas. (a) Reference flat map displaying cortical source voxels which comprise the primary cortical areas. BA 41 (Brodmann area 41) corresponds to primary auditory cortex. BA 1, 2, 3 (Brodmann areas 1, 2, 3) corresponds to primary somatosensory cortex. BA 17 (Brodmann area 17) corresponds to primary visual cortex. (b) Flat map of significantly different cortical sources across stimulation modalities (Quade test,  $p < 0.05$ ). Color-coding of voxels indicates the stimulation with the highest ranking based on the Quade test. Highest rank means the stimulation had the highest current relative to the other stimulation modalities. (c) Same as (b) except significant cortical source voxels are color-coded based on the *post hoc* procedures (Conover, 1999) for determining the significant comparison. Only comparisons where one stimulation modality is significantly larger than either or both of the other modalities are displayed. Note that there are significantly different cortical sources in left primary visual cortex for which the visual stimulation condition produces significantly higher relative currents compared to either auditory or somatosensory stimulation. A significantly different area also exists that includes the somatosensory cortices bilaterally but extends anteriorly to include supplemental motor areas. A, auditory; S, somatosensory; V, visual.

areas (Brodmann areas 6 and 8) bilaterally was also statistically different across stimulations and showed the largest relative currents when the K-complex was evoked by somatosensory stimulation. In contrast, relatively few areas showed differences where the highest relative current values during the negative peak of K-complexes were evoked by auditory tone stimulation.

The intriguing modality specificity of the cortical currents during the largest EEG component of the evoked slow wave prompted us to explore the time course of these current differences in K-complexes induced by peripheral stimulation. Therefore, we next examined the other

components of the evoked response, the P200, N350, and P900 time periods. The results of the Quade test for these two time periods are shown in Fig. 3. Like the K-complex negative peak, the P200 period includes significantly different cortical sources that include primary visual and somatosensory areas (Fig. 3). In addition, the rank and *post hoc* plots combine to show that stimulation causes a comparative increase in relative currents specific to the stimulation modality. That is, visual stimulation produced higher relative currents in visual cortex, while somatosensory stimulation was responsible for higher relative current in somatosensory cortices.



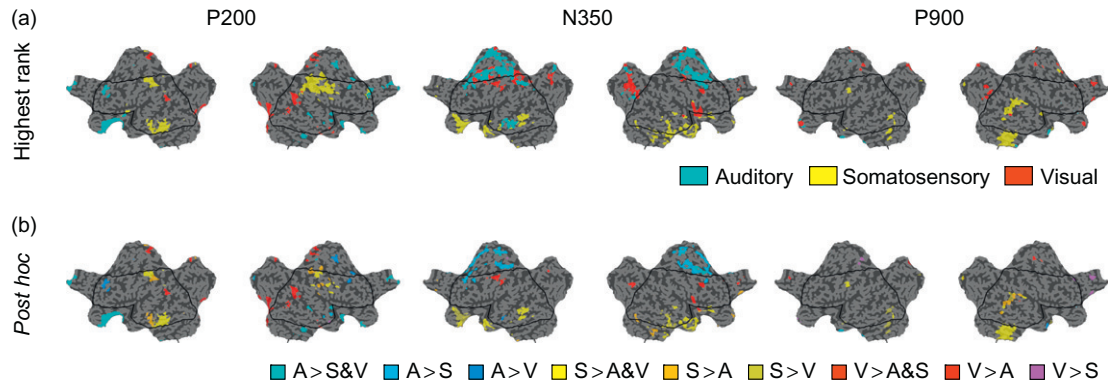


Fig. 3. The initial positive peak (P200), but not N350 or P900, shows modality specific differences in primary cortical areas. Same as Fig. 2 except that significantly different areas are shown for the three other components. For the P200 peak, both primary somatosensory and visual areas are significantly different based on the Quade test ( $p < 0.05$ ). The somatosensory and visual stimulations account for the most current in these areas, respectively (P200; a, b). The N350 peak shows significant areas in medial frontal, superior frontal, cingulate, and precuneus, but not the primary cortical areas. Few areas are significantly different during the P900.

Interestingly, the significant differences seemed to involve more circumscribed areas within the primary cortices than during the N550 peak, especially for sources ranking highest in the somatosensory condition. It should also be noted that there were cortical voxels that were significantly different outside of the primary cortical areas. For instance, parts of the inferior temporal cortex and fusiform gyri were significantly different showing increased current during somatosensory stimulation, although these areas are not generally thought to be involved in somatosensory information processing. The P200 time period comparison included some sizeable cortical areas where the significant differences across stimulation modality were being driven by auditory stimulation, including areas in the anterior cingulate, middle frontal, inferior frontal, and rectal gyri. These areas were among the highest in current for K-complexes in general, during both the negative peak and the P200 period (data not shown), regardless of stimulation. The finding that cortical areas specific for auditory stimulation are common to all K-complexes but are more strongly activated by tones, likely reflects the fact that

auditory stimulation is more effective in consistently evoking stereotypical slow waves. The fact that researchers often include a criterion for K-complex identification that includes a frontocentral maximum may also contribute to the reason why auditory stimulation is found to be more reliable (Colrain, 2005). Whether primary auditory cortex involvement is truly absent, is shorter in time than other stimulation modalities and thus more easily averaged over, or is an area that is particularly difficult to image with source modeling hd-EEG is unknown.

The modality specific differences during the P200 and N550 time periods may be a residual effect of the stimulation that fades over time. Thus, the further away in time from the stimulation, the less apparent the effect. However, the time period between the P200 and N550 K-complex peaks, which is labeled N350 in Fig. 1 and included an obvious negative component around this time in both the auditory and visual evoked responses, did not show significant differences in either somatosensory or visual primary cortical areas. The N350 component has often been attributed to vertex sharp waves (Colrain et al.,



2000). The lack of modality specific differences in primary cortical areas for the N350 peak, as there is in P200 and N550 time period suggests that the mechanisms underlying the production of vertex waves are indeed different in some distinct way from those involved in the K-complex, or at least do not show any reflection of primary sensory pathway involvement. In the P900 comparisons, there are relatively few cortical areas that are significantly different across conditions, and there is no apparent relationship with the primary sensory areas for either the visual or somatosensory conditions, as there was during the P200 and N550 component time periods.

These results confirm that during sleep, different types of stimuli evoke a stereotypic, global, and K-complex slow wave. However, the spatial and temporal resolution of source modeling hd-EEG allowed us to observe aspects of the evoked K-complex response that were not stereotypic. For somatosensory and visual stimulation, the P200 and the N550 components showed differential involvement of primary cortical areas consistent with the activation of primary sensory pathways. One possibility is that the global K-complex is produced by an initial activation of the primary cortical area that expands throughout the cortex via corticocortical connections or indirectly through other structures. An alternative explanation is that the evoked K-complex response reflects the parallel activation of both specific and nonspecific ascending sensory pathways to the cortex (Brodal, 1981). Specific pathways relay detailed sensory information to primary cortical areas, while the nonspecific pathways often involve collateral innervations of the reticular formation, and are capable of diffusely activating the entire cortex (Brodal, 1981; Jones, 2003). During sleep, the main function of the nonspecific pathways may be to provide an early warning signal of danger and potentially even wake the organism (Halasz et al., 2004). Thus, the stereotypical K-complex response common to all modalities of stimulation may be the result of nonspecific pathway involvement (Colrain, 2005) and the modality specific differential activations apparent in the

P200 and N550 components may result from parallel processing via the classical sensory pathways. This interpretation is consistent with the fact that auditory stimulation produces the most stereotypic K-complexes. In micro-osmotic animals, like humans, the auditory system is the most useful for detecting potential dangers in the environment during sleep and is therefore likely to be the most efficient in activating the nonspecific sensory pathways to produce the most stereotypical K-complex slow waves. While further investigations are needed to characterize the neural circuitry underlying these events, the hd-EEG data presented here suggest a previously unrecognized involvement of primary cortical areas at specific time periods during peripherally evoked slow waves.

## Conclusion

This chapter has focused on the various developments in analysis techniques that have been applied to slow waves in an attempt to understand their spatiotemporal dynamics. None of these techniques can be understood in isolation. Animal models have provided a comprehensive look at the underlying cellular mechanism—the slow oscillation. Intracranial recordings have confirmed the existence of the cortical slow oscillation in humans and have provided evidence for local slow waves. Noninvasive neuroimaging techniques with high spatial resolution have helped to delineate the cortical structures involved. Source modeling of hd-EEG fills an important gap in our understanding by attempting to explain the temporal dynamics which unfold with each slow wave. In addition to summarizing our previous results in the context of other techniques, we have addressed a long-standing assertion about the degree to which peripheral stimulation produces a nonspecific cortical slow wave in the brain during sleep. Through this demonstration we have discovered that at specific time periods peripherally evoked K-complexes do show primary sensory cortical activity related to the type of stimulation. These results highlight the power of

using hd-EEG in humans to examine slow waves in sleep and provide further evidence that the in-depth characterization of the spatial and temporal dynamics of slow waves in the sleeping human brain may represent a useful probe into the general functioning and connectivity of cortical circuits.

## Acknowledgments

Supported by the Neuroscience Training Program (NIHT9 DK070079), the Clinical Neuroengineering Training Program (NRSAT32 GM007507), the National Institute of Mental Health (P20MH077967), and funding provided by Philips-Respironics, Inc. We thank Simone Sarasso, Eric Landsness, and Yuval Nir for helpful discussions.

## References

- Amzica, F., & Steriade, M. (1995). Disconnection of intracortical synaptic linkages disrupts synchronization of a slow oscillation. *The Journal of Neuroscience*, *15*, 4658–4677.
- Amzica, F., & Steriade, M. (1997). The K-complex: Its slow (<1-Hz) rhythmicity and relation to delta waves. *Neurology*, *49*, 952–959.
- Amzica, F., & Steriade, M. (1998a). Cellular substrates and laminar profile of sleep K-complex. *Neuroscience*, *82*, 671–686.
- Amzica, F., & Steriade, M. (1998b). Electrophysiological correlates of sleep delta waves. *Electroencephalography and Clinical Neurophysiology*, *107*, 69–83.
- Bastien, C. H., Crowley, K. E., & Colrain, I. M. (2002). Evoked potential components unique to non-REM sleep: Relationship to evoked K-complexes and vertex sharp waves. *International Journal of Psychophysiology*, *46*, 257–274.
- Bastuji, H., & Garcia-Larrea, L. (1999). Evoked potentials as a tool for the investigation of human sleep. *Sleep Medicine Reviews*, *3*, 23–45.
- Berger, H. (1929). Über das Elektrenkephalogramm des Menschen (On the human electroencephalogram). *Archiv Fuer Psychiatrie Und Nervenkrankheiten*, *87*, 527–570.
- Blake, H., & Gerard, R. W. (1937). Brain potentials during sleep. *The American Journal of Physiology*, *119*, 692–703.
- Blake, H., Gerard, R. W., & Kleitman, N. (1939). Factors influencing brain potentials during sleep. *Journal of Neurophysiology*, *2*, 48–60.
- Born, A. P., Law, I., Lund, T. E., Rostrup, E., Hanson, L. G., Wildschiodt, G., et al. (2002). Cortical deactivation induced by visual stimulation in human slow-wave sleep. *NeuroImage*, *17*, 1325–1335.
- Brazier, M. A. (1949). The electrical fields at the surface of the head during sleep. *Electroencephalography and Clinical Neurophysiology*, *1*, 195–204.
- Brodal, A. (1981). *Neurological anatomy in relation to clinical medicine*. New York: Oxford University Press.
- Cash, S. S., Halgren, E., Dehghani, N., Rossetti, A. O., Thesen, T., Wang, C., et al. (2009). The human K-complex represents an isolated cortical down-state. *Science*, *324*, 1084–1087.
- Chauvette, S., Volgushev, M., & Timofeev, I. (2010). Origin of active states in local neocortical networks during slow sleep oscillation. *Cerebral Cortex*, *20*, 2660–2674.
- Colrain, I. M. (2005). The K-complex: A 7-decade history. *Sleep*, *28*, 255–273.
- Colrain, I., Webster, K., & Hirst, G. (1999). The N550 component of the evoked K-complex: A modality non-specific response? *Journal of Sleep Research*, *8*, 273–280.
- Colrain, I. M., Webster, K. E., Hirst, G., & Campbell, K. B. (2000). The roles of vertex sharp waves and K-complexes in the generation of N300 in auditory and respiratory-related evoked potentials during early stage 2 NREM sleep. *Sleep*, *23*, 97–106.
- Conover, W. J. (1999). *Practical nonparametric statistics*. New York: Wiley.
- Contreras, D., & Steriade, M. (1995). Cellular basis of EEG slow rhythms—A study of dynamic corticothalamic relationships. *The Journal of Neuroscience*, *15*, 604–622.
- Crunelli, V., & Hughes, S. (2010). The slow (<1 Hz) rhythm of non-REM sleep: A dialogue between three cardinal oscillators. *Nature Neuroscience*, *13*, 9–17.
- Czisch, M., Wehrle, R., Stiegler, A., Peters, H., Andrade, K., Holsboer, F., et al. (2009). Acoustic oddball during NREM sleep: A combined EEG/fMRI study. *PloS One*, *4*, 11.
- Czisch, M., Wetter, T. C., Kaufmann, C., Pollmacher, T., Holsboer, F., & Auer, D. P. (2002). Altered processing of acoustic stimuli during sleep: Reduced auditory activation and visual deactivation detected by a combined fMRI/EEG study. *NeuroImage*, *16*, 251–258.
- Dang-Vu, T., Desseilles, M., Laureys, S., Degueldre, C., Perrin, F., Phillips, C., et al. (2005). Cerebral correlates of delta waves during non-REM sleep revisited. *NeuroImage*, *28*, 14–21.
- Dang-Vu, T., Schabus, M., Desseilles, M., Albouy, G., Boly, M., Darsaud, A., et al. (2008). Spontaneous neural activity during human slow wave sleep. *Proceedings of the National Academy of Sciences of the United States of America*, *105*, 15160–15165.
- Davis, H., Davis, P. A., Loomis, A. L., Harvey, E. N., & Hobart, G. (1938). Human brain potentials during the onset of sleep. *Journal of Neurophysiology*, *1*, 24–38.

- Davis, H., Davis, P. A., Loomis, A. L., Harvey, E. N., & Hobart, G. (1939). Electrical reactions of the human brain to auditory stimulation during sleep. *Journal of Neurophysiology*, 2, 500–514.
- Destexhe, A., Contreras, D., & Steriade, M. (1999). Spatio-temporal analysis of local field potentials and unit discharges in cat cerebral cortex during natural wake and sleep states. *The Journal of Neuroscience*, 19, 4595–4608.
- Garcia, S., Fernandez, A., Luengo, J., & Herrera, F. (2010). Advanced nonparametric tests for multiple comparisons in the design of experiments in computational intelligence and data mining: Experimental analysis of power. *Information Sciences (New York)*, 180, 2044–2064.
- Gastaut, H., Naquet, R., Vigouroux, R., Roger, A., & Badier, M. (1953). Electrographic studies in man and in animal in so-called psychomotor epilepsy. *Revue Neurologique (Paris)*, 88, 310–354.
- Gotman, J. (2003). Noninvasive methods for evaluating the localization and propagation of epileptic activity. *Epilepsia*, 44(Suppl. 12), 21–29.
- Hagmann, P., Cammoun, L., Gigandet, X., Meuli, R., Honey, C. J., Wedeen, V., et al. (2008). Mapping the structural core of human cerebral cortex. *PLoS Biology*, 6, 1479–1493.
- Halasz, P., Terzano, M., Parrino, L., & Bodizs, R. (2004). The nature of arousal in sleep. *Journal of Sleep Research*, 13, 1–23.
- Hamalainen, M., Hari, R., Ilmoniemi, R. J., Knuutila, J., & Lounasmaa, O. V. (1993). Magnetoencephalography—Theory, instrumentation, and applications to noninvasive studies of the working human brain. *Reviews of Modern Physics*, 65, 413–497.
- Hennevin, E., Huetz, C., & Edeline, J. (2007). Neural representations during sleep: From sensory processing to memory traces. *Neurobiology of Learning and Memory*, 87, 416–440.
- Hofle, N., Paus, T., Reutens, D., Fiset, P., Gotman, J., Evans, A., et al. (1997). Regional cerebral blood flow changes as a function of delta and spindle activity during slow wave sleep in humans. *The Journal of Neuroscience*, 17, 4800–4808.
- Issa, E., & Wang, X. (2008). Sensory responses during sleep in primate primary and secondary auditory cortex. *The Journal of Neuroscience*, 28, 14467–14480.
- Jones, B. E. (2003). Arousal systems. *Frontiers in Bioscience*, 8, S438–S451.
- Kaufmann, C., Wehrle, R., Wetter, T. C., Holsboer, F., Auer, D. P., Pollmacher, T., et al. (2006). Brain activation and hypothalamic functional connectivity during human non-rapid eye movement sleep: An EEG/fMRI study. *Brain*, 129, 655–667.
- Loomis, A. L., Harvey, E. N., & Hobart, G. A. III (1938). Distribution of disturbance-patterns in the human electroencephalogram, with special reference to sleep. *Journal of Neurophysiology*, 1, 413–430.
- Lopes Da Silva, F. (2004). Functional localization of brain sources using EEG and/or MEG data: Volume conductor and source models. *Magnetic Resonance Imaging*, 22, 1533–1538.
- Maquet, P. (2000). Functional neuroimaging of normal human sleep by positron emission tomography. *Journal of Sleep Research*, 9, 207–231.
- Massimini, M., Huber, R., Ferrarelli, F., Hill, S., & Tononi, G. (2004). The sleep slow oscillation as a traveling wave. *The Journal of Neuroscience*, 24, 6862–6870.
- Massimini, M., Rosanova, M., & Mariotti, M. (2003). EEG slow (approximately 1 Hz) waves are associated with non-stationarity of thalamo-cortical sensory processing in the sleeping human. *Journal of Neurophysiology*, 89, 1205–1213.
- Michel, C., Murray, M., Lantz, G., Gonzalez, S., Spinelli, L., & Grave De Peralta, R. (2004). EEG source imaging. *Clinical Neurophysiology*, 115, 2195–2222.
- Millett, D. (2001). Hans Berger—From psychic energy to the EEG. *Perspectives in Biology and Medicine*, 44, 522–542.
- Mohajerani, M. H., Mcvea, D. A., Fingas, M., & Murphy, T. H. (2010). Mirrored bilateral slow-wave cortical activity within local circuits revealed by fast bihemispheric voltage-sensitive dye imaging in anesthetized and awake mice. *The Journal of Neuroscience*, 30, 3745–3751.
- Murphy, M., Riedner, B., Huber, R., Massimini, M., Ferrarelli, F., & Tononi, G. (2009). Source modeling sleep slow waves. *Proceedings of the National Academy of Sciences of the United States of America*, 106, 1608–1613.
- Nir, Y., Staba, R. J., Andrillon, T., Vyazovskiy, V. V., Cirelli, C., Fried, I., & Tononi, G. (2011). Regional Slow Waves and Spindles in Human Sleep. *Neuron*, 70, 153–169.
- Nofzinger, E. (2005). Functional neuroimaging of sleep. *Seminars in Neurology*, 25, 9–18.
- Nofzinger, E. A., Buysse, D. J., Miewald, J. M., Meltzer, C. C., Price, J. C., Sembrat, R. C., et al. (2002). Human regional cerebral glucose metabolism during non-rapid eye movement sleep in relation to waking. *Brain*, 125, 1105–1115.
- Nunez, P., & Srinivasan, R. (2005). *Electric fields of the brain: The neurophysics of EEG*. New York, USA: Oxford University Press.
- Pascual-Marqui, R. D. (2002). Standardized low-resolution brain electromagnetic tomography (sLORETA): Technical details. *Methods and Findings in Experimental and Clinical Pharmacology*, 24, 5–12.
- Portas, C. M., Krakow, K., Allen, P., Josephs, O., Armony, J. L., & Frith, C. D. (2000). Auditory processing across the sleep-wake cycle: Simultaneous EEG and fMRI monitoring in humans. *Neuron*, 28, 991–999.
- Raichle, M. E., Macleod, A. M., Snyder, A. Z., Powers, W. J., Gusnard, D. A., & Shulman, G. L. (2001). A default mode of brain function. *Proceedings of the*

- National Academy of Sciences of the United States of America*, 98, 676–682.
- Raichle, M., & Snyder, A. (2007). A default mode of brain function: A brief history of an evolving idea. *NeuroImage*, 37, 1083–1090.
- Rosanov, M., & Timofeev, I. (2005). Neuronal mechanisms mediating the variability of somatosensory evoked potentials during sleep oscillations in cats. *The Journal of Physiology*, 562, 569–582.
- Roth, M., Shaw, J., & Green, J. (1956). The form voltage distribution and physiological significance of the K-complex. *Electroencephalography and Clinical Neurophysiology*, 8, 385–402.
- Steriade, M., Jones, E. G., & Llinás, R. R. (1990). *Thalamic oscillations and signaling*. New York: Wiley.
- Steriade, M., Nuñez, A., & Amzica, F. (1993a). A novel slow (<1 Hz) oscillation of neocortical neurons in vivo: Depolarizing and hyperpolarizing components. *The Journal of Neuroscience*, 13, 3252–3265.
- Steriade, M., Nuñez, A., & Amzica, F. (1993b). Intracellular analysis of relations between the slow (<1 Hz) neocortical oscillation and other sleep rhythms of the electroencephalogram. *The Journal of Neuroscience*, 13, 3266–3283.
- Steriade, M., Timofeev, I., & Grenier, F. (2001). Natural waking and sleep states: A view from inside neocortical neurons. *Journal of Neurophysiology*, 85, 1969–1985.
- Timofeev, I., Grenier, F., Bazhenov, M., Sejnowski, T. J., & Steriade, M. (2000). Origin of slow cortical oscillations in deafferented cortical slabs. *Cerebral Cortex*, 10, 1185–1199.
- Timofeev, I., & Steriade, M. (1996). Low-frequency rhythms in the thalamus of intact-cortex and decorticated cats. *Journal of Neurophysiology*, 76, 4152–4168.
- Velluti, R. (1997). Interactions between sleep and sensory physiology. *Journal of Sleep Research*, 6, 61–77.
- Volgushev, M., Chauvette, S., Mukovski, M., & Timofeev, I. (2006). Precise long-range synchronization of activity and silence in neocortical neurons during slow-wave oscillations. *The Journal of Neuroscience*, 26, 5665–5672.
- von Helmholtz, H. L. F. (2004). Some laws concerning the distribution of electric currents in volume conductors with applications to experiments on animal electricity (English translation). *Proceedings of the Institute of Electrical and Electronics Engineers*, 92, 868–870.
- Vyazovskiy, V. V., Olcese, U., Lazimy, Y. M., Faraguna, U., Esser, S. K., Williams, J. C., et al. (2009). Cortical firing and sleep homeostasis. *Neuron*, 63, 865–878.
- Wennberg, R. (2010). Intracranial cortical localization of the human K-complex. *Clinical Neurophysiology*, 121, 1176–1186.